Direct Kinetic Correlation of Carriers and Ferromagnetism in Co^{2+}: ZnO

Kevin R. Kittilstved,[1] Dana A. Schwartz,[1] Allan C. Tuan,[2] Steve M. Heald,[2] Scott A. Chambers,[2] and Daniel R. Gamelin[1,*]

[1]*Department of Chemistry, University of Washington, Seattle, Washington, 98195, USA*
[2]*Pacific Northwest National Laboratory, Richland, Washington, 99352, USA*

(Received 18 May 2006; published 19 July 2006)

The hypothesis that high-Curie-temperature ferromagnetism in cobalt-doped ZnO (Co^{2+}: ZnO) is mediated by charge carriers was tested by controlled introduction and removal of the shallow donor interstitial zinc. Using oriented epitaxial Co^{2+}: ZnO films grown by chemical vapor deposition, kinetics measurements demonstrate a direct correlation between the oxidative quenching of ferromagnetism and the diffusion and oxidation of interstitial zinc. These results demonstrate controlled systematic variation of a key parameter involved in the ferromagnetism of Co^{2+}: ZnO and, in the process, unambiguously reveal this ferromagnetism to be dependent upon charge carriers. The distinction between defect-bound and free carriers in Co^{2+}: ZnO is discussed.

DOI: 10.1103/PhysRevLett.97.037203 PACS numbers: 75.50.Pp, 71.55.−i, 75.30.−m, 81.15.Gh

In only a few cases have the key factors controlling long-range magnetic ordering in diluted magnetic semiconductors (DMSs) been unambiguously identified. In $Ga_{1-x}Mn_xAs$, the identification and variation of critical experimental parameters has culminated in a testable microscopic model describing hole-mediated magnetic ordering in this and several related manganese-doped III-V semiconductors [1]. The recent discovery of high-Curie-temperature (T_C) ferromagnetism in doped oxide semiconductors has stimulated intense experimental and theoretical interest in these materials [2]. In contrast with $Ga_{1-x}Mn_xAs$, a clear consensus has not yet been reached about the relationship between carriers (bound or free) and ferromagnetism in these doped oxides. Only through identification and systematic variation of key compositional parameters will a significant advance in the understanding of high-T_C ferromagnetism in doped oxides be realized.

In this Letter, we demonstrate that the native shallow donor interstitial zinc (Zn_i) is capable of activating high-T_C ferromagnetism in Co^{2+}-doped ZnO (Co^{2+}: ZnO). The Zn_i concentration in an oriented epitaxial thin film of Co^{2+}: ZnO was systematically varied by controlled oxidative removal of these shallow donors at elevated temperatures. A direct correlation between the 300 K ferromagnetic saturation moment (M_S) and the concentration of Zn_i was observed. The experimental activation barriers clearly identify the diffusion of Zn_i as the rate-determining process in the oxidative quenching of ferromagnetism in Co^{2+}: ZnO. These results provide conclusive evidence that the high-T_C ferromagnetism in Co^{2+}: ZnO is mediated by donor-bound carriers.

Metal-organic chemical vapor deposition epitaxial growth and characterization of Co^{2+}: ZnO films on *r*-plane α-Al_2O_3 was reported previously [3]. Additional details are provided as supplementary information [4]. Figure 1 shows the 300 K electronic absorption spectrum of a 9% Co^{2+}: ZnO film in its insulating form (resistivity, $R > 10^2\ \Omega\,cm$). The electronic absorption and magnetic circular dichroism (MCD) spectroscopies of this paramagnetic Co^{2+}: ZnO film have been reported previously [3]. Zn vapor diffusion into Co^{2+}: ZnO was performed as described in Ref. [5]. After annealing the film in zinc vapor at 600 °C for 5 hours, the resistivity dropped by over 3 orders of magnitude to ~0.1 Ω cm and changes were observed in the electronic absorption spectrum. Specifically, a new transition in the IR region and a concomitant blueshift of the band edge by ~68 meV were observed upon exposure to Zn vapor, both signatures of donors in ZnO [5,6]. Moss-Burstein analysis [7] of the band edge shift places the donor concentration in the range of $N = 5 \times 10^{18}\ cm^{-3}$, similar to those estimated for other ZnO samples annealed under Zn vapor [5,8] and ca. 10^2 times

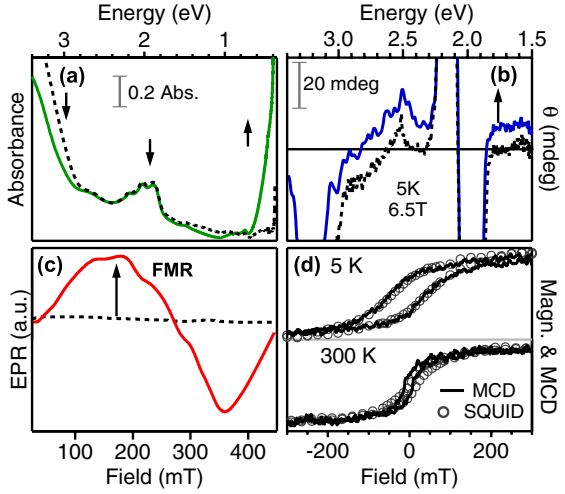

FIG. 1 (color online). Spectroscopic and magnetic data for 9% Co^{2+}: ZnO epi film: (a) 300 K electronic absorption spectra of Co^{2+}: ZnO (dashed line) and Zn_i: Co^{2+}: ZnO (solid line). (b) 5 K, 6.5 T MCD spectra [same legend as in (a)]. (c) 300 K EPR spectra [same legend as in (a)]. Arrows indicate the spectral changes upon exposure to Zn metal vapor. (d) 5 (top) and 300 K (bottom) MCD intensity at 1.77 eV (solid line) and magnetic susceptibility (○) plotted versus the applied magnetic field for Zn_i: Co^{2+}: ZnO.

smaller than the Co^{2+} concentration. This donor concentration corresponds to the intermediate doping regime of $Na^3 = 0.06$ (where $a = 2.31$ nm is the effective Bohr radius of the Zn_i-bound carrier [9]).

Annealing in Zn vapor was found to activate partial ferromagnetic ordering in the film [Fig. 1(d) and Ref. [4]]. The relatively small saturation moment [$M_S(300\ K) \approx 0.1\mu_B/Co^{2+}$] is commensurate with the small ratio of Zn_i to Co^{2+} and the small fraction (~30%) of Co^{2+} ions that do not have antiferromagnetically coupled nearest neighbor Co^{2+} ions at this relatively high Co^{2+} concentration (9%). The 5 and 300 K MCD spectra of the Zn_i: Co^{2+}: ZnO film exhibited new positive intensity spanning the entire visible energy range [Fig. 1(b)], similar to that reported previously for polycrystalline Zn_i: Co^{2+}: ZnO [10]. The 5 and 300 K magnetization curves collected while monitoring this new MCD intensity display clear ferromagnetic hystereses with coercivities that are similar to those measured by SQUID magnetometry on the same film [~80 Oe at 300 K, ~400 Oe at 5 K; see Fig. 1(d) and Ref. [4]]. This broad featureless MCD intensity is attributed to low energy photoionization transitions from a ferromagnetic spin-split Co^{2+}/Zn_i impurity band [10]. The ferromagnetic ground state of Zn_i: Co^{2+}: ZnO also displayed a so-called ferromagnetic resonance at 300 K that was not observed in the paramagnetic form [Fig. 1(c)]. As described previously [5], the spectroscopic, magnetic, and conductivity changes induced by Zn vapor diffusion are all quantitatively reversed by brief aerobic oxidation (10 minutes at 600 °C), indicating the Zn_i perturbation is nondestructive. The similarity between these data and those reported for polycrystalline Co^{2+}: ZnO demonstrates that the effects described here are independent of the structural form or source of the Co^{2+}: ZnO DMS.

The electronic structures of Co^{2+}: ZnO and Zn_i: Co^{2+}: ZnO epitaxial films were investigated by cobalt and zinc K-shell x-ray absorption spectroscopy (XAS). These spectra were first collected on Zn_i: Co^{2+}: ZnO and then recollected on the same film after aerobic reoxidization. As shown in Fig. 2(a), the Co K-edge spectra of Co^{2+}: ZnO and Zn_i: Co^{2+}: ZnO both show the signature $1s \rightarrow 3d$ pre-edge absorption of substitutional Co^{2+} in ZnO at ca. 7709 eV. The pre-edge and edge regions of the Co^{2+}: ZnO and Zn_i: Co^{2+}: ZnO XAS spectra are superimposable, indicative of little change in electron density at the Co^{2+} upon Zn vapor diffusion. For comparison, metallic cobalt shows a distinct broad K-edge absorption feature at ca. 7712 eV that is not present in the spectra of Co^{2+}: ZnO or Zn_i: Co^{2+}: ZnO. Fourier transforms of the extended fine structure (EXAFS) from the XAS data [Fig. 2(b)] provide further evidence that there is no change in the Co^{2+} speciation upon Zn vapor diffusion. The scattering lengths obtained from analysis of the cobalt [Fig. 2(b)] and zinc [Fig. 2(b)] EXAFS data are identical for both Co^{2+}: ZnO and Zn_i: Co^{2+}: ZnO (see [4]). Notably absent from the cobalt EXAFS data [Fig. 2(b)] is any intensity at the Co-Co nearest neighbor distance of cobalt metal (2.5 Å) [11]. These data rule out phase segregation as the source of the Co^{2+}: ZnO ferromagnetism induced by Zn vapor diffusion and instead point to an intrinsic origin.

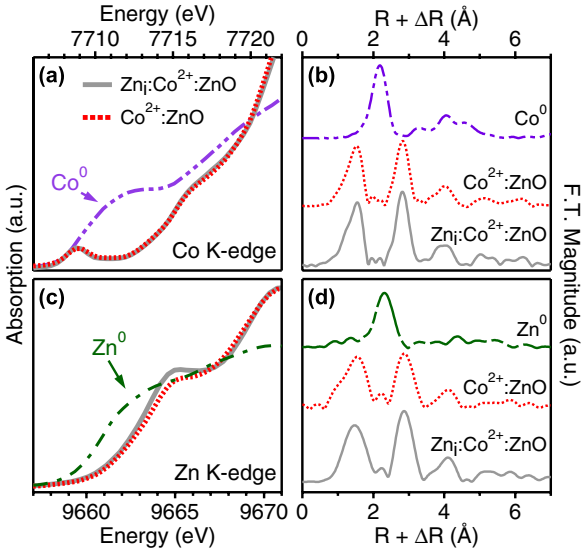

FIG. 2 (color online). X-ray absorption data for 9% Co^{2+}: ZnO epi film: (a) Co and (c) Zn K-edge x-ray absorption spectra of Co^{2+}: ZnO (dashed red line) and Zn_i: Co^{2+}: ZnO (solid line). Data for cobalt metal and zinc metal are shown in (a) and (c), respectively, for comparison. (b) and (d) show Fourier transforms of the EXAFS data for Co^{2+}: ZnO and Zn_i: Co^{2+}: ZnO. Reference transforms are shown for cobalt metal in (b) and zinc metal in (d).

The Zn K-edge XAS and EXAFS data for both Co^{2+}: ZnO and Zn_i: Co^{2+}: ZnO in Fig. 2(c) also show the expected features of Zn^{2+} in ZnO. There is, however, a notable increase in intensity at 9665 eV upon introduction of Zn_i. It is tempting to attribute this intensity directly to K-shell absorption of Zn_i, but further experiments are required before such an assignment can be made conclusively.

The data in Fig. 3(a) demonstrate quantitatively reversible cycling of the 300 K conductivity, M_S, and IR absorption intensity between Co^{2+}: ZnO and Zn_i: Co^{2+}: ZnO by alternating Zn vapor diffusion and aerobic oxidation. Approximately 50 cycles have been performed on this film without any detectable material decomposition or loss of reproducibility. Although these data strongly suggest a correlation between conductivity, Zn_i, and ferromagnetism in Co^{2+}: ZnO, they do not necessarily demonstrate a causal relationship between Zn_i and ferromagnetism. To test for causality, the *kinetics* of the interconversion between "on" and "off" forms were examined. To our knowledge, there have been no previous reports describing the kinetics of magnetic phase transitions in high-T_C doped oxides.

The oxidative phase transition is rapid at 600 °C but can be slowed by reducing the oxidation temperature. Oxida-

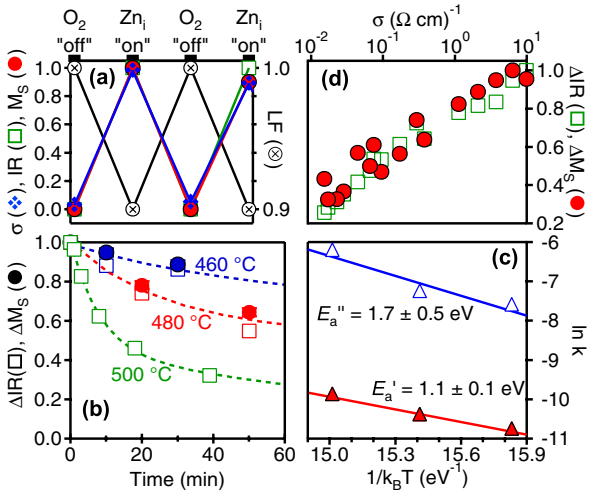

FIG. 3 (color online). (a) Quantitatively reversible cycling of M_S(300 K) (solid red circles), conductivity (σ, blue diamonds), IR absorbance (□), and ligand field absorption (⊗) for a 9% Co^{2+}: ZnO film with alternating air ("off") and Zn vapor ("on") annealing. (b) Kinetic decay curves for M_S(300 K) (solid circles) and IR intensities (squares) versus oxidation time at 460, 480, and 500 °C for the same film. Best fit double-exponential decay curves are shown as dashed lines. (c) Natural logs of the two rate constants plotted versus inverse thermal energy. The linear slopes yield the activation energies indicated. (d) 300 K M_S and IR absorbance versus the log of the film's 300 K conductivity for data from (b).

tion kinetics measurements were therefore performed at 460, 480, and 500 °C for 35, 5.8, and 2.7 hours, respectively. The initial decay data are plotted in Fig. 3(b). The decays of M_S(300 K) and the IR intensity are clearly correlated, both showing similar double-exponential decay kinetics that accelerate the same way as the temperature is elevated. Such kinetic correlation can occur only if the ferromagnetism and IR absorption are associated with the same species. Furthermore, when the data from Fig. 3(b) are plotted versus the film conductivity on a logarithmic scale, a clear linear relationship is observed for both M_S(300 K) and the IR intensity [see Fig. 3(d)]. Combined, these data demonstrate unambiguously a direct causal relationship between ferromagnetism and carriers in Co^{2+}: ZnO. We note that, in the course of this oxidation, the conductivity drops by 3 orders of magnitude as the film is converted from intermediate to light Zn_i doping ranges (Na^3 decreases from ca. 0.06 to 0), but there is no evidence for reduction of T_C to below 300 K.

Figure 3(c) plots the decay rate constants from the data in Fig. 3(b) versus the inverse thermal energy for each oxidation temperature. Straight lines are obtained for both the fast and slow rate components, indicating Arrhenius behavior. The biphasic decay kinetics yield two activation energies for oxidative quenching of ferromagnetism: $E_a' = 1.1 \pm 0.1$ eV and $E_a'' = 1.7 \pm 0.5$ eV. These values are in excellent agreement with those reported previously for the diffusion of Zn_i in ZnO, which range from 0.87 to 1.52 eV for temperatures between 375 and 940 °C [12]. The two activation barriers observed here may be related to (i) Zn_i diffusion through the lattice to the surface and (ii) more rapid diffusion along grain boundaries, both followed by rapid oxidation at the ZnO/air interface. Importantly, these low activation barriers are consistent with diffusion of interstitial zinc (a non-Frenkel lattice defect) but not with diffusion of oxygen vacancies (V_O), which requires displacement of substitutional anions. Literature activation energies for oxygen diffusion in ZnO are much larger than those in Fig. 3(c) (e.g. >5.0 eV for bulk ZnO, ~3.1 eV for polycrystalline ZnO, and ~3.4 eV for polycrystalline Co^{2+}: ZnO [13]). The data in Fig. 3 thus provide strong evidence that Zn_i, and not V_O, is the defect responsible for the ferromagnetism in Co^{2+}: ZnO described here.

Recently, we related the ferromagnetism of TM^{2+}: ZnO to the charge-transfer electronic structures of the TM^{2+} ions [9]. Shallow donors such as Zn_i are energetically aligned with the $Co^{+/2+}$ level leading to effective dopant-defect hybridization as described by perturbation theory. Here we focus on the important distinction between bound and free charge carriers. The data in Fig. 3 demonstrate conclusively that carriers introduced by Zn_i activate ferromagnetism in Co^{2+}: ZnO, an observation consistent with formation of a shallow spin-split Zn_i/Co^{2+} impurity band [5,9,10,14]. Formation of such a band upon coalescence of bound magnetic polarons in oxide DMSs has been described theoretically [14]. A possible alternative mechanism for carrier-mediated magnetic ordering in Co^{2+}: ZnO is the Ruderman-Kittel-Kasuya-Yosida (RKKY) or related Zener mechanism, in which itinerant free carriers interact with localized d electrons on isolated dopant ions. The RKKY mechanism has recently been proposed to be the dominant mechanism behind ferromagnetic ordering in Co^{2+}: TiO_2 and related oxide DMSs at elevated temperatures [15].

Recent results from various laboratories have suggested that high-T_C ferromagnetism in Co^{2+}: ZnO can be achieved through the introduction of shallow bound carriers in the form of grain-boundary defects [16,17] or oxygen substoichiometries [3,5,18]. In the former, aerobic aggregation of paramagnetic TM^{2+}: ZnO nanocrystals at room temperature induced partial ferromagnetic ordering attributed to introduction of nonstoichiometric grain-boundary defects at nanocrystal-nanocrystal fusion interfaces [16,19]. Since aggregation was performed at room temperature, this result suggests that there is no intrinsic barrier to ferromagnetic ordering in Co^{2+}: ZnO once appropriate defects are introduced.

The direct relationship between M_S(300 K) and the shallow donor concentration (Fig. 3) provides conclusive evidence that ferromagnetism in Co^{2+}: ZnO is carrier dependent. The steep relationship between the Co^{2+}: ZnO film's conductivity and both M_S(300 K) and the concentration of Zn_i [$\log\sigma \propto N$ (or M_S); Fig. 3(d) and Ref. [4]] is

similar to the relationship between conductivity and donor concentration predicted by percolation theory for hopping conductivity ($\log\sigma \propto N^{-1/3}$ [20]). The data in Fig. 3(d) thus suggest that delocalized free carriers and metallic conductivity are not required for room-temperature ferromagnetism in Co^{2+}: ZnO and, hence, that this ferromagnetism does not arise from the RKKY mechanism. This conclusion is consistent with the strong temperature dependence of conductivity in the intermediate doped Co^{2+}: ZnO films despite a ferromagnetic saturation moment that is relatively temperature independent over the same temperature range (5–300 K) [4,21]. Combined, these results argue for an important role played by the Zn_i defect itself, particularly at low Zn_i concentrations where the film is insulating. Defect-bound carriers may differ from free carriers in important ways, including in their extent of hybridization with magnetic dopants [9], in their potential to adopt triplet ground state configurations [14,22], and in their capacity to stabilize magnetic polarons [23]. By implicating defect-bound carriers, the data in Fig. 3 support a description of ferromagnetism in Zn_i: Co^{2+}: ZnO involving bound magnetic polarons.

In summary, carrier-mediated high-T_C ferromagnetism in Co^{2+}: ZnO has been demonstrated unambiguously by controlled introduction and removal of the shallow donor Zn_i under conditions where the kinetics of the magnetic phase transition could be monitored and analyzed. M_S(300 K) was found to be correlated quantitatively with shallow donor IR absorption in Co^{2+}: ZnO, both displaying the same biphasic oxidation kinetics. The activation barriers for the oxidative quenching of ferromagnetism are identical to those for Zn_i diffusion in ZnO, identifying the shallow donor Zn_i as the key mediating defect in ferromagnetic Co^{2+}: ZnO prepared in this way. These results advance our understanding of high-T_C ferromagnetism in oxide DMSs by demonstrating controlled systematic variation of a key parameter involved in the ferromagnetism of Co^{2+}: ZnO, namely, the Zn_i concentration.

This work was funded by the U.S. National Science Foundation (DMR-0239325 to D. R. G.), the Research Corporation, the Dreyfus Foundation, and the Sloan Foundation. Work at the Environmental Molecular Sciences Laboratory (a national scientific user facility sponsored by the U.S. DOE's Office of Biological and Environmental Research and located at Pacific Northwest National Laboratory) was supported by the U.S. DOE Office of Science, Division of Materials Sciences and Engineering. Use of the Advanced Photon Source was supported by the U.S. DOE under Contract No. W-31-109-ENG-38.

*Electronic address: Gamelin@chem.washington.edu

[1] T. Jungwirth, K. Y. Wang, J. Masek, K. W. Edmonds, J. Konig, J. Sinova, M. Polini, N. A. Goncharuk, A. H. MacDonald, M. Sawicki, A. W. Rushforth, R. P. Campion, L. X. Zhao, C. T. Foxon, and B. L. Gallagher, Phys. Rev. B **72**, 165204 (2005); H. Ohno, Science **281**, 951 (1998); T. Dietl, H. Ohno, F. Matsukura, J. Cibert, and D. Ferrand, Science **287**, 1019 (2000).

[2] For a recent review, see C. Liu, F. Yun, and H. Morkoç, J. Mater. Sci.: Mater. Electron. **16**, 555 (2005).

[3] A. C. Tuan, J. D. Bryan, A. B. Pakhomov, V. Shutthanandan, S. Thevuthasan, D. E. McCready, D. Gaspar, M. H. Engelhard, J. W. Rogers, Jr., K. Krishnan, D. R. Gamelin, and S. A. Chambers, Phys. Rev. B **70**, 054424 (2004).

[4] See EPAPS Document No. E-PRLTAO-97-033630 for supplementary materials consisting of experimental details and additional magnetic and spectroscopic data. For more information on EPAPS, see http://www.aip.org/pubservs/epaps.html.

[5] D. A. Schwartz and D. R. Gamelin, Adv. Mater. **16**, 2115 (2004).

[6] D. G. Thomas, Phys. Chem. Solids **3**, 229 (1957); R. M. de la Cruz, R. Pareja, R. González, L. A. Boatner, and Y. Chen, Phys. Rev. B **45**, 6581 (1992).

[7] E. Burstein, Phys. Rev. **93**, 632 (1954); T. S. Moss, Proc. Phys. Soc. London, Sect. B **67**, 775 (1954); H. Fujiwara and M. Kondo, Phys. Rev. B **71**, 075109 (2005).

[8] L. E. Halliburton, N. C. Giles, N. Y. Garces, M. Luo, C. Xu, L. Bai, and L. A. Boatner, Appl. Phys. Lett. **87**, 172108 (2005).

[9] K. R. Kittilstved, W. K. Liu, and D. R. Gamelin, Nat. Mater. **5**, 291 (2006).

[10] K. R. Kittilstved, J. Zhao, W. K. Liu, J. D. Bryan, D. A. Schwartz, and D. R. Gamelin, cond-mat/0507121.

[11] C. Kittel, *Introduction to Solid State Physics* (Wiley, New York, 1996), 7th ed.

[12] E. Gebhardt, Z. Mattlkd. **37**, 87 (1946); A. Krupkowski and S. Balicki, Met. Corros. **12**, 89 (1937); W. J. Moore and J. K. Lee, Trans. Faraday Soc. **47**, 501 (1951); E. A. Secco, J. Chem. Phys. **29**, 406 (1958).

[13] H. Haneda, I. Sakaguchi, A. Watanabe, T. Ishigaki, and J. Tanaka, J. Electroceram. **4**, S41 (1999).

[14] J. M. D. Coey, M. Venkatesan, and C. B. Fitzgerald, Nat. Mater. **4**, 173 (2005).

[15] M. J. Calderón and S. D. Sarma, cond-mat/0603182.

[16] D. A. Schwartz, N. S. Norberg, Q. P. Nguyen, J. M. Parker, and D. R. Gamelin, J. Am. Chem. Soc. **125**, 13 205 (2003).

[17] A. Fouchet, W. Prellier, and B. Mercey, cond-mat/0604468.

[18] M. Venkatesan, C. B. Fitzgerald, J. G. Lunney, and J. M. D. Coey, Phys. Rev. Lett. **93**, 177206 (2004); N. Khare, M. J. Kappers, M. Wei, and M. G. Blamire, Adv. Mater. **18**, 1449 (2006).

[19] P. V. Radovanovic and D. R. Gamelin, Phys. Rev. Lett. **91**, 157202 (2003).

[20] B. I. Shklovskii and A. L. Efros, *Electronic Properties of Doped Semiconductors* (Springer-Verlag, Berlin, 1984).

[21] A. B. Pakhomov, B. K. Roberts, A. Tuan, V. Shutthanandan, D. McCready, S. Thevuthasan, S. A. Chambers, and K. M. Krishnan, J. Appl. Phys. **95**, 7393 (2004).

[22] C. H. Patterson, cond-mat/0512101.

[23] P. A. Wolff, in *Semiconductors and Semimetals*, edited by J. K. Furdyna and J. Kossut (Academic, San Diego, 1988), Vol. 25, p. 413.